
Erik Jonsson School of Engineering and Computer Science

2012-07-11

Effect of Acetylene Concentration and Thermal Ramping Rate on the Growth of Spin-capable Carbon Nanotube Forests

Kyung H. Lee, *et al.*

© 2012 American Vacuum Society

Further information may be found at: [http:// libtreasures.utdallas.edu/xmlui/handle/10735.1/2500](http://libtreasures.utdallas.edu/xmlui/handle/10735.1/2500)

Effect of acetylene concentration and thermal ramping rate on the growth of spin-capable carbon nanotube forests

Kyung H. Lee, Dae Woong Jung, Dorothea Burk, Lawrence J. Overzet, and Gil S. Lee

Citation: *J. Vac. Sci. Technol. B* **30**, 041809 (2012); doi: 10.1116/1.4736985

View online: <http://dx.doi.org/10.1116/1.4736985>

View Table of Contents: <http://avspublications.org/resource/1/JVTBD9/v30/i4>

Published by the AVS: Science & Technology of Materials, Interfaces, and Processing

Related Articles

Fluorine-Doped Iron Oxide Nanomaterials by Plasma Enhanced-CVD: An XPS Study
Surf. Sci. Spectra **20**, 9 (2013)

Synthesis, properties, and applications of silicon nanocrystals
J. Vac. Sci. Technol. B **31**, 020801 (2013)

Field emission from nanometer-scale tips of crystalline $\text{PbZr}_x\text{Ti}_{1-x}\text{O}_3$
J. Vac. Sci. Technol. B **31**, 021805 (2013)

Optimization of a self-closing effect to produce nanochannels with top slits in fused silica
J. Vac. Sci. Technol. B **30**, 06FF09 (2012)

Fabrication of silicon nanopore arrays using a combination of dry and wet etching
J. Vac. Sci. Technol. B **30**, 061804 (2012)

Additional information on *J. Vac. Sci. Technol. B*

Journal Homepage: <http://avspublications.org/jvstb>

Journal Information: http://avspublications.org/jvstb/about/about_the_journal

Top downloads: http://avspublications.org/jvstb/top_20_most_downloaded

Information for Authors: http://avspublications.org/jvstb/authors/information_for_contributors

ADVERTISEMENT

Instruments for advanced science

Gas Analysis



- dynamic measurement of reaction gas streams
- catalysis and thermal analysis
- molecular beam studies
- dissolved species probes
- fermentation, environmental and ecological studies

Surface Science



- UHV TPD
- SIMS
- end point detection in ion beam etch
- elemental imaging - surface mapping

Plasma Diagnostics



- plasma source characterization
- etch and deposition process reaction kinetic studies
- analysis of neutral and radical species

Vacuum Analysis



- partial pressure measurement and control of process gases
- reactive sputter process control
- vacuum diagnostics
- vacuum coating process monitoring

contact Hiden Analytical for further details

HIDEN ANALYTICAL

info@hideninc.com
www.HidenAnalytical.com

CLICK to view our product catalogue 

Effect of acetylene concentration and thermal ramping rate on the growth of spin-capable carbon nanotube forests

Kyung H. Lee, Dae Woong Jung, Dorothea Burk, Lawrence J. Overzet, and Gil S. Lee^{a)}
The University of Texas at Dallas, Department of Electrical Engineering, 800 W. Campbell Road, Richardson,
Texas 75080

(Received 22 December 2011; accepted 26 June 2012; published 11 July 2012)

Spin-capable multiwalled carbon nanotube (MWCNT) forests that can form webs, sheets, and yarns provide a promising means for advancing various technologies. It is necessary to understand the critical factors to grow spin-capable carbon nanotubes (CNTs) in a repeatable fashion. Here we show how both the spinning capability and morphology of MWCNT forests are significantly changed by controlling the C_2H_2 concentration and ramp rate of temperature. The acetylene gas flow was varied in the range of 0.25–6.94% by volume. The MWCNTs grown at C_2H_2 concentrations between 1.47–3.37% are well-aligned and become spin-capable. The well-aligned forests have higher areal density and shorter distance between CNTs. The thermal ramp rate was also changed from 30 °C/min to 70 °C/min. A specific range of thermal ramp rate is also required to have the suitably sized nanoparticles with sufficient density resulting in higher CNT areal density for spinnable MWCNTs. A ramp rate of 50 °C/min forms suitable sized nanoparticles with sufficient density to produce CNT forests with a higher areal density and a shorter tube spacing. © 2012 American Vacuum Society. [<http://dx.doi.org/10.1116/1.4736985>]

I. INTRODUCTION

While spin-capable carbon nanotubes (CNTs) that form CNT sheets and/or yarns have attracted great interest because they have enabled many advanced technologies such as nanostructured electrode materials for energy storage,^{1–3} sensors,⁴ and polymer composite materials with reinforced mechanical strength,⁵ the important factors enabling the growth of the spin-capable forests are still not well-known. It was reported that growing of spin-capable CNTs forests depends on several growth factors such as catalyst film thickness, growth temperature, and carrier and reactant gases.^{6–10} The other factors still remain to be investigated more thoroughly to date. These include flow rate (or ratio) of reactant gas, reactant gas species, and pressure. We showed¹⁰ that the spinning capability depends on the alignment of adjacent CNTs in a forest, which in turn results from the combination of a high areal density of CNTs and short distance between the CNTs. This could be realized by starting with both the proper Fe nanoparticle size and density which strongly depend on the thickness of Fe film. In addition, it was demonstrated¹¹ that the reduction of the native iron oxide in as-deposited Fe films suppresses the formation of contiguous films, helping to form nanoparticles which provide nucleation sites for CNTs which are well-aligned and spin-capable. Jayasinghe *et al.*¹² reported spinnable long CNT forests with 4–6 mm height which was one of the hot issues to increase electrical, physical, and mechanical property. They also showed that the spinability decreased at high partial pressure of ethylene. It needs to be investigated further.

To understand the other factors for growth of spin-capable CNT forests, our research interest has been centered on how the growth behavior of MWCNTs is affected by

acetylene (C_2H_2) gas and thermal ramping rate. Here we show how the spinning capability and morphology of MWCNT forests are significantly changed by controlling C_2H_2 concentration and thermal ramping rate.

II. EXPERIMENT

CNTs were grown from iron films, which were deposited by electron-beam evaporation onto Si substrates with an oxidized layer of thickness 400 nm. The thickness of the Fe films was 5 nm and was monitored by a quartz-crystal sensor fixed inside the e-beam evaporation chamber. The CNT growth was performed in cold wall CVD system including a quartz and stainless steel cylindrical CVD chamber (chamber diameter of 120 mm, gap of 15 mm between a shower head of 25 mm diameter and a heater block) at atmospheric pressure using flows of a mixture of C_2H_2 , He, and H_2 gas. The substrate was introduced into the CVD chamber and ramped to the set point temperature of 780 °C at a ramping rate of 50 °C/min while flowing He [20 standard liter per minute (slm)] and H_2 (100 sccm). The growth of CNTs was then carried out at the same temperature and pressure by adding C_2H_2 gas to the flow for 5 min. The C_2H_2 gas flow was varied in the range of 50 to 1500 sccm (0.25% to 6.94% by volume of the total flow). After completing the growth of CNTs, the sample was cooled to below 100 °C in the same H_2 /He gas mixture. In addition, we changed the ramping rate from 30 °C/min to 70 °C/min. The CNTs were grown at 780 °C for 5 min in gas mixture of He (20 slm), H_2 (100 sccm), and C_2H_2 (400 sccm) with 30 °C/min, 50 °C/min, and 70 °C/min condition, respectively.

The CNTs were characterized by scanning electron microscopy (SEM, ZEISS SUPRA 40, 1530VP), Raman spectroscopy (JY HORIBA, LAB RAM Raman HR), and transmission electron microscopy (TEM, JEOL, 2100). The areal density of CNTs was calculated by directly counting the holes resulting from pulling out CNTs from the substrate.

^{a)} Author to whom correspondence should be addressed; electronic-mail: gslee@utdallas.edu

III. RESULTS AND DISCUSSION

A. Effect of acetylene

The height of CNT forests increased from $100\ \mu\text{m}$ to $330\ \mu\text{m}$ as C_2H_2 concentration increased from 0.25 to 1.47%, corresponding to the growth rate of 0.3 and $1.0\ \mu\text{m/s}$, respectively (Fig. 1). The forest height remains unchanged in

the range of 1.47 to 4.74%. The further increase of C_2H_2 concentration (6.94%) makes the height decrease to $140\ \mu\text{m}$ again. A higher concentration of acetylene decreased the lifetime of catalyst because it resulted in a deactivation of catalyst particles possibly by forming a carbon byproduct on the surface of particles.¹³ A low acetylene concentration caused a low carbon concentration after decomposition of

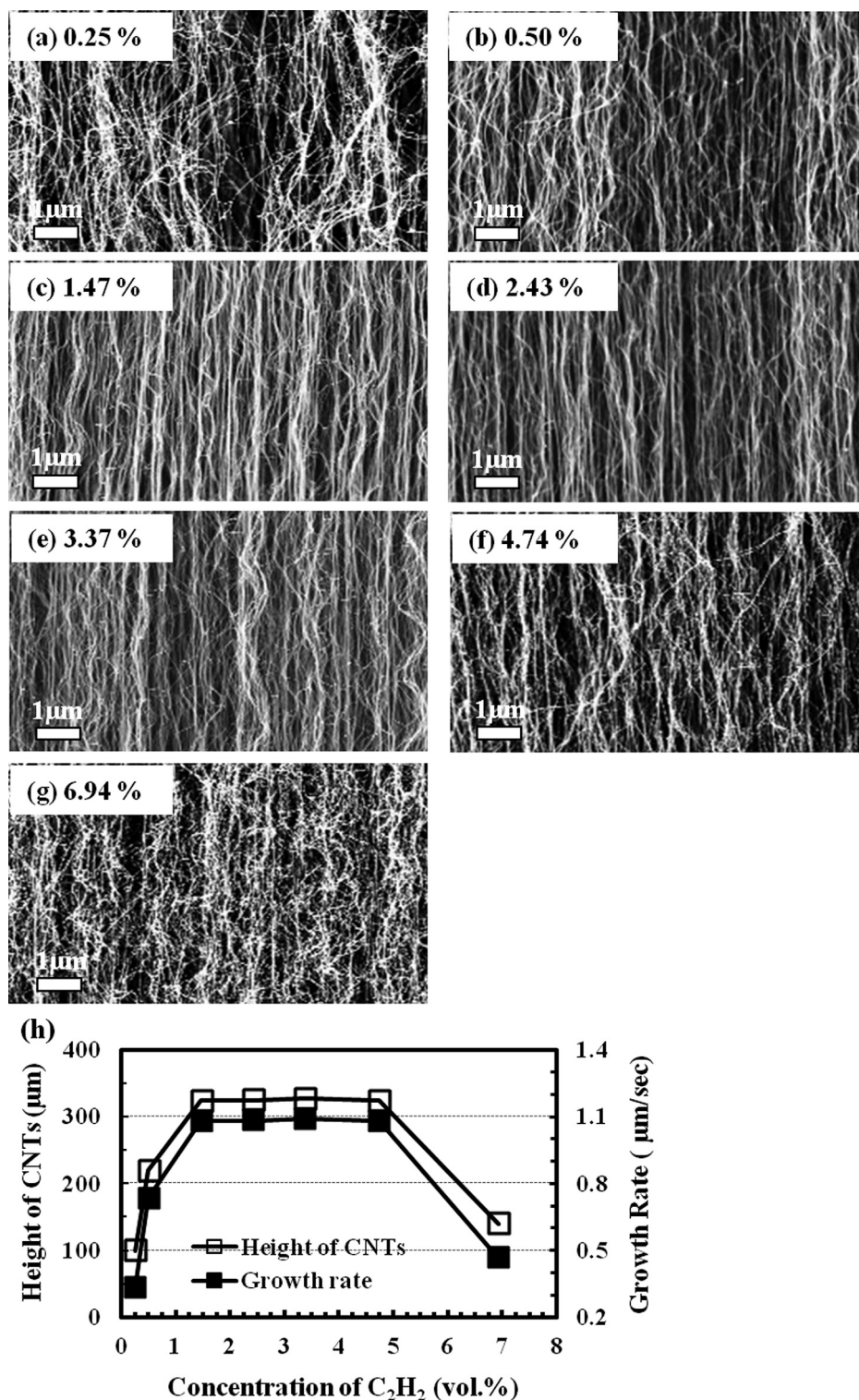


Fig. 1. High resolution SEM images of MWCNTs grown at different concentration of acetylene to show different alignment. (a) 0.25, (b) 0.5, (c) 1.47, (d) 2.43, (e) 3.37, (f) 4.74, (g) 6.94 vol. %, and (h) a graph of the forest height dependence on the acetylene concentration.

acetylene at the surface of catalyst particles resulting in the short height of CNTs.¹⁴

Figure 1 consists of SEM images of the MWCNTs in seven forests grown at various concentrations of C_2H_2 . When the concentration of C_2H_2 is 0.25%, the CNTs appear wavy or curled. As the concentration of C_2H_2 increases from 0.25% to 2.43%, the alignment of CNT forests is improved, forming CNTs that are well-aligned. The further increase of C_2H_2 concentration to 6.94% worsens the alignment of CNTs, resulting in curled or wavy forests again. As a result, the C_2H_2 concentration between 1.47% and 3.37% makes CNTs appear dense and well-aligned. On the contrary, the CNTs grown both at the highest concentration of 6.94% and the lowest concentration of 0.25% appear the most curled. This alignment is strongly dependent on the acetylene concentration. In agreement with our previous reports¹⁰ that CNT sheets and/or yarns can be pulled from the well-aligned CNT forests, the CNT forests grown at the

acetylene concentration between 1.47% and 3.37% become spin-capable, forming more than 3 m long sheets or yarns. The others are not spin-capable. This indicates that the spinning capability of CNT forests is strongly dependent on the concentration of C_2H_2 .

To understand the dependence of the spinning capability on the C_2H_2 concentration, the CNT diameter and its distribution were investigated by TEM (Fig. 2). Regardless of C_2H_2 concentration, all of the CNTs were MWCNTs, which is consistent with the Raman spectra of the CNTs (Fig. 3). Histograms of the average diameters and standard deviation with Gaussian fitting are shown in Fig. 2. The average CNT diameter grown at C_2H_2 concentration of 0.25–4.74% is around 12.23 ± 1.6 – 13.11 ± 1.5 nm, but is slightly higher (14.22 ± 1.1 nm) at 6.94%. This indicates that the CNT diameter does not change significantly as the C_2H_2 concentration is increased. It is in good agreement with a previous result from Hasegawa *et al.*¹³ They

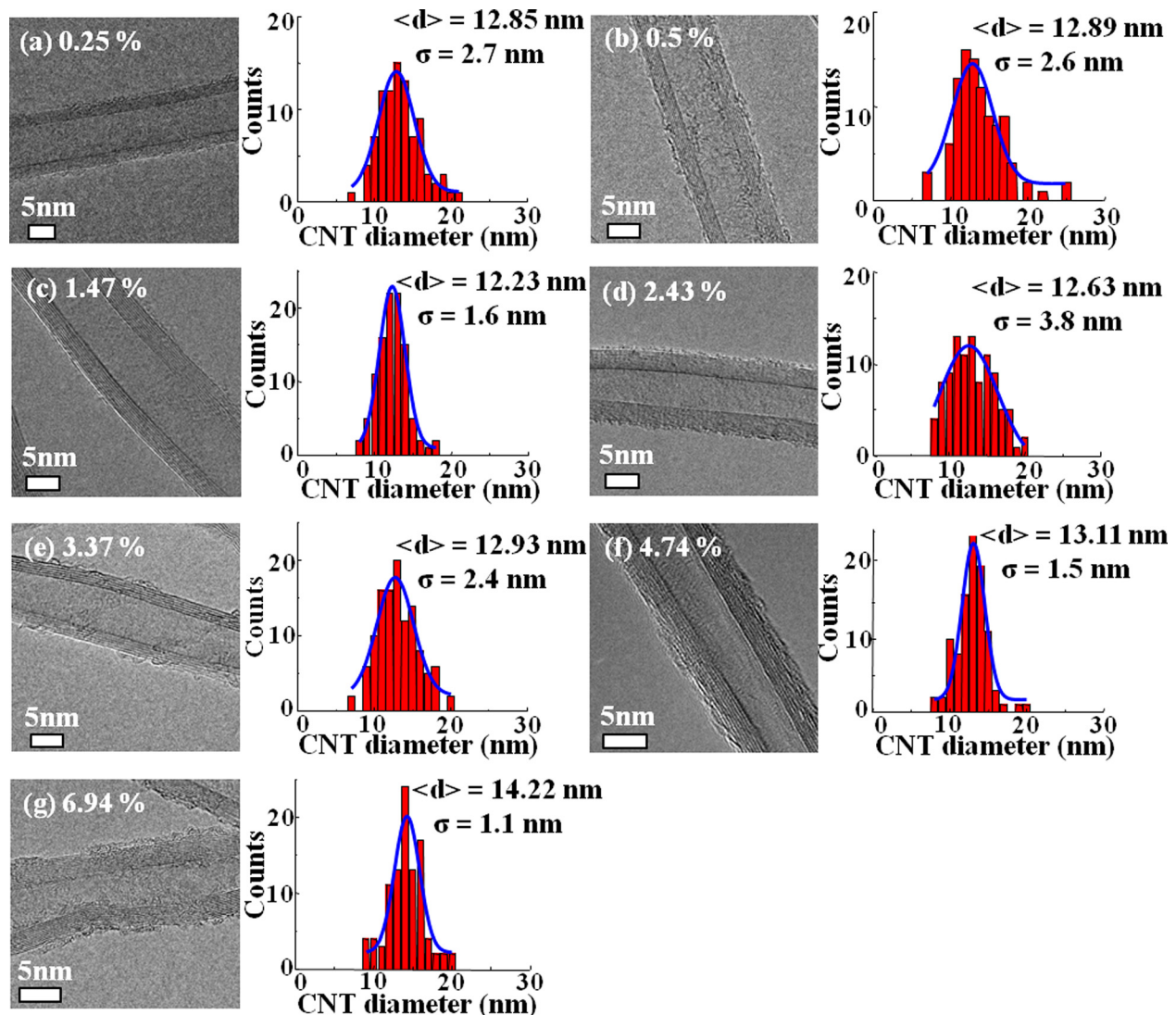


Fig. 2. (Color online) TEM images and histograms of the average diameters (and the standard deviation) of the CNTs associated with various acetylene concentration with Gaussian fitting (red solid lines). (a) 0.25, (b) 0.5, (c) 1.47, (d) 2.43, (e) 3.37, (f) 4.74, and (g) 6.94 vol. % of acetylene.

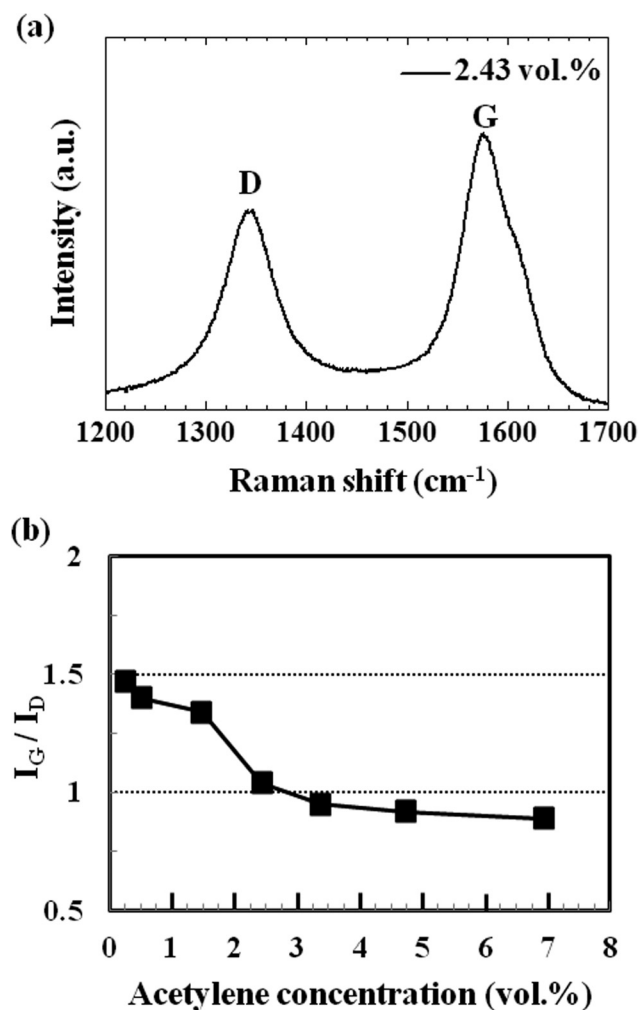


Fig. 3. Raman spectra of MWCNT grown at 2.43% of C₂H₂ (a) and I_G/I_D of CNTs grown at various acetylene concentration (b).

reported that the diameter of CNTs grown on the same thickness of Fe catalyst film remained unchanged at different acetylene concentrations but correlated with catalyst particle size.

To examine the spinning capability (or the alignment) depending on the C₂H₂ concentration in more detail, the average distance between adjacent CNTs (tube spacing) was estimated using the average CNTs diameter and the areal density (Fig. 4). The well-aligned CNTs grown at 1.47–3.37% have an areal density greater than 1.2×10^{10} tubes/cm², but the others have lower areal density. As expected, the tube spacing for 1.5–3.5% is smaller than that for the others by 20–30 nm as shown in Fig. 4. As a result, the CNTs grown at the C₂H₂ concentrations of 1.47–3.37% have a larger areal density (narrower tube spacing), and form well-aligned and spin-capable CNT forests.^{9,10}

Interestingly, the ratio of intensity between G peak and D peak (G/D) ratio obtained by Raman spectra of the MWCNT forests (Fig. 3) decreases from 1.47 to 0.89 as the C₂H₂ concentration increases from 0.25% to 6.94%. This means that the MWCNTs may have more defects and/or a larger amount of amorphous carbon as the C₂H₂ concentration increases. In

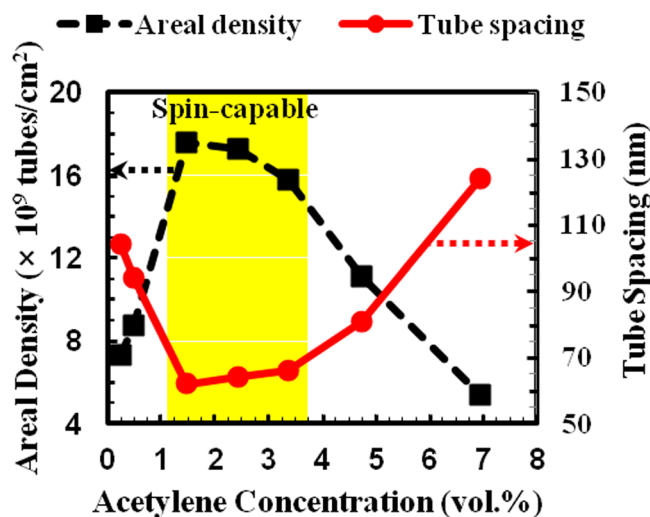


Fig. 4. (Color online) Plots of areal density of CNT forests (black dash line) and tube spacing (red solid line) between adjacent CNTs as a function of acetylene concentration.

addition, amorphous carbon is clearly observed on the surface of CNTs grown at the higher C₂H₂ concentration of both 4.74 and 6.94% as can be seen in TEM images. This is consistent with the decreased G/D peak ratio at higher C₂H₂ concentration in Raman results. We also believe that the increase of the amorphous carbon at the highest C₂H₂ concentration causes the CNTs to be shorter in height due to early deactivation of the Fe catalyst (Fig. 1).

B. Thermal ramping rate

Carbon nanotube synthesis depends upon the morphology and activity of metal catalysts.¹⁰ Fe catalyst film thickness is critical to form proper sized nanoparticles which cause spin-capable CNT forests.¹⁰ Thermal ramping rate is one of key factors to grow spin-capable CNT forests. The ramping rate is the time at which the sample is raised from room temperature to growth temperature (780 °C). Spin-capable CNT growth was investigated as a function of different ramp rates ranging from 30 °C/min to 70 °C/min, with the process conditions fixed at 780 °C and mixture of 100 sccm H₂, 400 sccm C₂H₂, and 20 slm He.

Figure 5 shows high resolution SEM images of CNT forests grown at different ramping rates and a plot of growth height as a function of ramp rate. As shown at Fig. 5(d), the highest height of the CNT forest is 400 μm at 50 °C/min, while the height are 360 μm and 250 μm at 30 and 70 °C/min, respectively. High resolution SEM images show relationship between thermal ramp rate and CNTs alignment. The CNT forests morphology grown at three different conditions show a big difference. Spinnable CNT forests [Fig. 5(b)] grown at 50 °C/min condition in super-aligned arrays have a much better alignment than nonspinnable CNTs grown at 30 °C/min [Fig. 5(a)] and 70 °C/min [Fig. 5(c)]. The morphologies of CNTs grown at 70 °C/min show undulating shape where the curvature increases with thermal ramp rate. Thermal ramp rate of 50 °C/min results in good alignment and spin-capability.

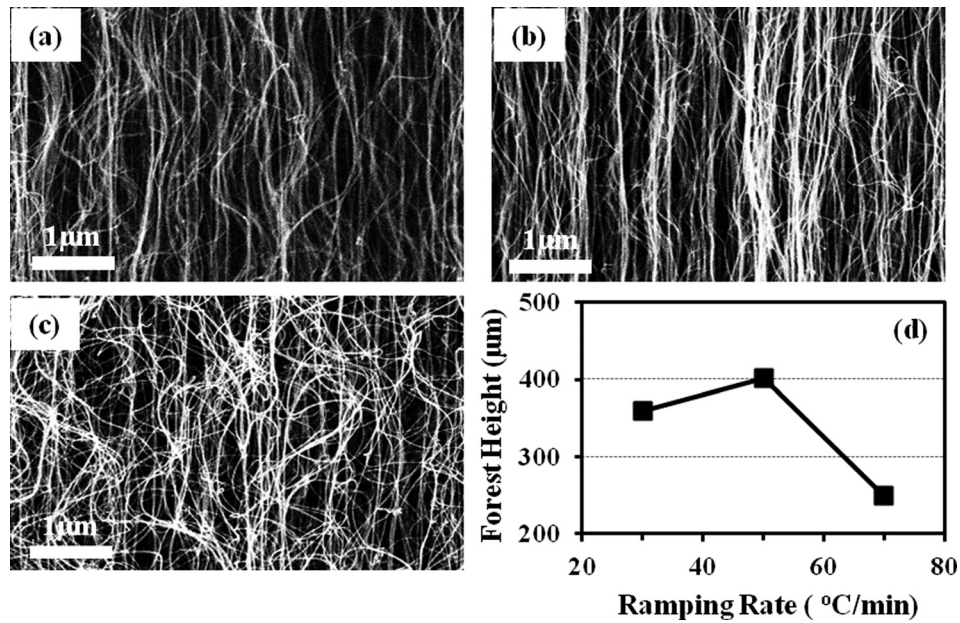


Fig. 5. High resolution SEM images of MWCNT forests grown at different ramping rate and plot of growth height as a function of ramping rate. (a) 30 °C/min, (b) 50 °C/min, (c) 70 °C/min, and (d) a graph of the forest height dependence on the ramping rate.

The average CNT diameter measured by TEM decreased as ramping rate increased as shown in Fig. 6. The average diameter of CNT is 13.4 ± 2.69 nm, 12.5 ± 2.14 nm, and 11.7 ± 2.27 nm when the ramp rate is 30 °C/min, 50 °C/min, and 70 °C/min, respectively. This indicates that different ramp rates produce different diameter catalytic nanoparticles and CNTs. It is well-known that small/large catalytic nanoparticles form small/large diameter of CNTs.¹⁵

The areal density of CNT forests grown with different ramp rate is also shown in Fig. 6. The areal density of the CNT forests grown at 50 °C/min condition which are spin-capable are greater than 1.8×10^{10} tubes/cm², while CNTs grown at 30 °C/min and 70 °C/min have an areal density less than 1.5×10^{10} tubes/cm². When the ramping rate is 30 °C/min and

70 °C/min, the Fe catalyst films do not generate enough Fe nanoparticles suitable for spin-capable CNTs.

The average distance between adjacent CNTs is around 62 nm for spin-capable CNT forests grown at 50 °C/min condition. Others have an average distance higher than 70 nm. As a result, the ramp rate of 50 °C/min forms CNT forests which have higher areal density and shorter tube spacing and causes that CNT forests produce CNT sheet and yarns.

To validate these results, SEM was used to characterize the morphology of catalyst particles. Figure 7 shows SEM images of the catalyst films that have undergone pretreatment with different ramp rates. The average size of Fe nanoparticles are 14.1 ± 2.83 nm, 12.6 ± 3.25 nm, and 11.7 ± 2.40 nm for 30 °C/min, 50 °C/min, and 70 °C/min ramp rates. We find that Fe nanoparticle size corresponds to the diameters of CNTs approximately. It is well-known that the size of catalyst particles has an important influence on the diameter of CNTs.¹⁵

In addition, for the same thickness Fe catalytic film different ramp rate cause the film to break into small/large size nanoparticles. Slow ramp rates like 30 °C/min form large particles at low density due to the Ostwald ripening phenomena.¹⁶ The long ramp time of 30 °C/min provides high thermal energy to the Fe nanoparticles which diffuse or migrate along the surface to neighboring nanoparticles. The resulting larger nanoparticles having the lower density afford fewer nucleation sites for growth of carbon nanotubes and lead to the low areal density and the curled morphology of these CNT forests. On the other hand, Fe particles formed in fast ramping rate like 70 °C/min condition form small, sparse isolated islands, too few for sufficient nucleation sites. They result in low areal density, curled CNT forests. We found that a specific range of ramp rate is required to have the suitably sized nanoparticles with sufficient density resulting in higher CNT areal density for spinnable MWCNTs.

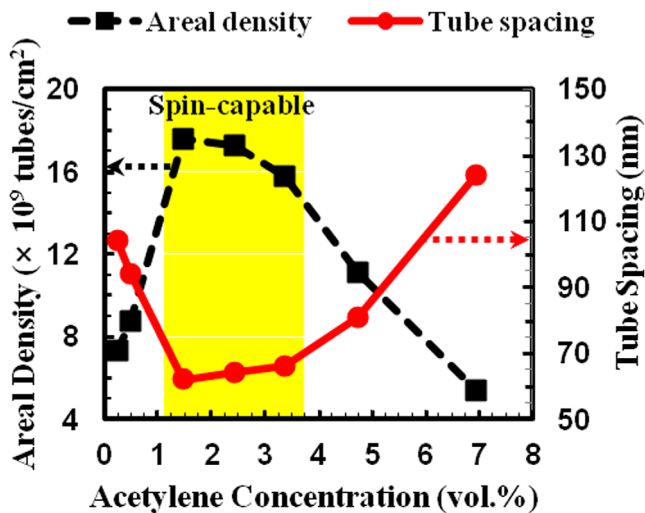


Fig. 6. (Color online) Plots of areal density of CNT forests (black dashed line), CNTs average diameter (blue dotted line), and tube spacing (red solid line) between adjacent CNTs as a function of thermal ramping rate.

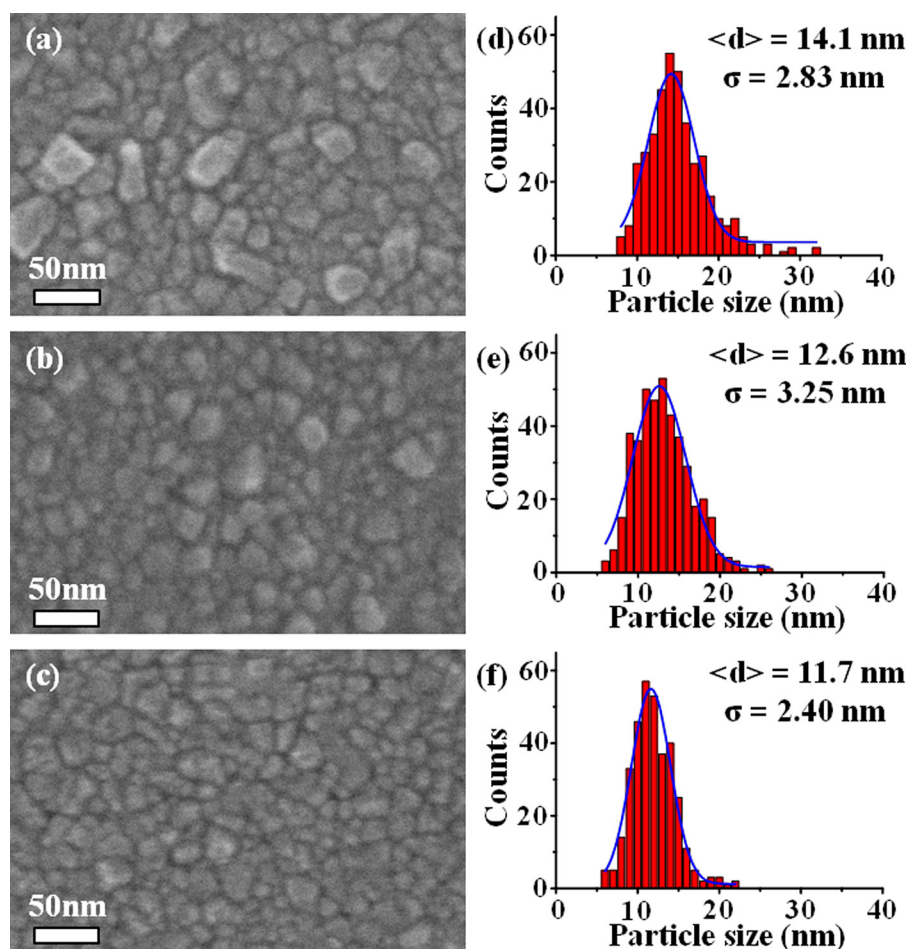


Fig. 7. (Color online) SEM images showing the surface morphology of catalyst films that have undergone pretreatment with different ramping rate and particle size distribution. (a) and (d) 30 °C/min, (b) and (e) 50 °C/min, (c) and (f) 70 °C/min.

IV. CONCLUSIONS

We have investigated the relationship between the spinning capability of CNT forests and the concentration of C_2H_2 and the ramp rate of temperature. The spinning capability of CNT forests strongly depends on the concentration of C_2H_2 and thermal ramp rates. Spin-capable MWCNT forests grow successfully in C_2H_2 concentrations between 1.47% and 3.37%. CNT forests grown at this concentration range are well-aligned, have a higher areal density (or shorter distance between adjacent CNTs) and have less amorphous carbon while other CNTs grown outside this range of C_2H_2 are more curled and have lower areal density. As a result, either insufficient or excess carbon in the source gas leads to decreasing the areal density, which results in poorer alignment of CNTs and spinning capability of the forests. A specific range of thermal ramp rate is also required to have the suitably sized nanoparticles with sufficiently higher CNT areal density for spinnable MWCNTs. A ramp rate of 50 °C/min forms suitable sized nanoparticles with sufficient density to produce CNT forests with a higher areal density and shorter tube spacing. Slower or faster ramp rates (30 °C/min and 70 °C/min) make small/large catalytic nanoparticles and then provide fewer nucleation sites resulting in poorer CNTs density, and curled and nonspinnable CNT forests.

ACKNOWLEDGMENT

This research was supported by DMS contract at the University of Texas at Dallas.

- ¹A. L. M. Reddy, M. M. Shaijumon, S. R. Gowda, and P. M. Ajayan, *Nano Lett.* **9**, 1002 (2009).
- ²M. D. Lima *et al.*, *Science* **331**, 51 (2001).
- ³H. Zhang, G. Cao, Z. Wang, Y. Yang, Z. Shi, and Z. Gu, *Nano Lett.* **8**, 2664 (2008).
- ⁴M. Musameh, M. R. Notivoli, M. Hickey, I. L. Kyratzis, Y. Gao, H. Chi, and C. H. Stephen, *Adv. Mater.* **23**, 906 (2011).
- ⁵M. in het Panhuis, *J. Mater. Chem.* **16**, 3598 (2006).
- ⁶M. Zhang, K. R. Atkinson, and R. H. Baughman, *Science* **306**, 1358 (2004).
- ⁷X. Zhang, K. Jiang, C. Feng, P. Liu, L. Zhang, and J. Kong, *Adv. Mater.* **18**, 1505 (2006).
- ⁸X. Zhang, Q. Li, L. Tu, Y. Li, J. Y. Coulter, and L. Zheng, *Small* **3**, 244 (2007).
- ⁹K. Liu, Y. Sun, L. Chen, C. Feng, X. Feng, and K. Jiang, *Nano Lett.* **8**, 700 (2008).
- ¹⁰J.-H. Kim, H.-S. Jang, K. H. Lee, L. J. Overzet, and G. S. Lee, *Carbon* **48**, 538 (2010).
- ¹¹J.-H. Kim, K. H. Lee, D. Burk, L. J. Overzet, and G. S. Lee, *Carbon* **48**, 4301 (2010).
- ¹²C. Jayasinghe, S. Chakrabarti, M. J. Schulz, and V. Shanov, *J. Mater. Res.* **26**, 645 (2011).
- ¹³K. Hasegawa and S. Noda, *ACS Nano* **5**, 975 (2011).
- ¹⁴F. Ahmadzade, S. Safa, and P. Balashabady, *Arabian J. Sci. Eng.* **36**, 97 (2011).
- ¹⁵B. Zhao, D. N. Futaba, S. Yasuda, M. Akoshima, T. Yamada, and K. Hata, *ACS Nano* **3**, 108 (2009).
- ¹⁶M. Jose-Yacamán, C. Gutierrez-Wing, M. Miki, D. Z. Yang, K. N. Piyakis, and E. Sacher, *J. Phys. Chem. B.* **109**, 9703 (2002)